Journal Name

ARTICLE

Catechol oxidase activity of comparable dimanganese and dicopper complexes

Adriana M. Magherusan, Daniel N. Nelis, Brendan Twamley, Aidan R. McDonald*

Received 00th January 20xx,
Accepted 00th January 20xx

DOI: 10.1039/x0xx00000x

www.rsc.org/

Synthetic dicopper complexes have been widely investigated as model systems for catechol oxidase enzymes. The catechol oxidase reactivity of dimanganese complexes has been less explored, and the effect of metal substitution in catecholase mimics has not been explored. A series of Mn^{II}_2 and Cu^{II}_2 complexes supported by the same poly-benzimidazole ligand framework have been synthesised and investigated in catecholase activity in acetonitrile medium using 3,5-di-*tert*-butylcatechol (3,5-DTBC) as a substrate. The Cu^{II}_2 complexes proved to be good catechol oxidase mimics with moderate k_{cat} values (~45 h^{-1}). The kinetic parameters for Mn^{II}_2 complexes exhibited lower k_{cat} values (~8-40 h^{-1}) when compared to the Cu^{II}_2 complexes. Our findings demonstrate that later transition metals supported by relatively electron rich ligands yield the highest k_{cat} values for catechol oxidation.

Introduction

Catechol oxidase, a type-3 Cu protein, uses a process known as catecholase activity to catalyse the oxidation of *o*-diphenols (catechols) to the corresponding quinones. One of the key roles of catechol oxidases is to maintain disease resistance in plants, to protect damaged tissue against pathogens and insects.[1] Moreover the conversion of the catechol to the quinone is very important in medical diagnosis for the determination of the hormonal catecholamines adrenaline, noradrenaline, and dopa.[2, 3]

A variety of biomimetic catalysts that mimic the catechol oxidase activity have been explored in order to get a better understanding of the active site and mechanism of reaction of these Cu proteins.[4-10] Recently Mn complexes have emerged for studying the catecholase activity even though no Mn containing catechol oxidase enzyme has been discovered to date.[11-14] The postulated mechanism of catechol oxidase and Cu synthetic models action is the reduction of Cu^{II} to Cu^{I} by the catechol, inducing oxidation to the quinone product.[4, 6-9] For Mn, Ni, and Zn mimics, EPR (electron paramagnetic resonance) experiments showed the generation of radicals when complexes were reacted with catechol. Thus a mechanism involving a radical pathway has been proposed for these systems.[15, 16 17 18] We were interested in exploring further the role of the metal ion in catechol oxidase reactivity. Specifically, we wanted to explore the relative effects of exchanging Mn for Cu in the same ligand environment and the effect of employing an early transition metal (Mn) versus a late transition metal (Cu) in catechol oxidation.

Besides the catechol oxidases, we maintain a keen interest in the analogous class Ib Mn_2 ribonucleotide reductases (RNRs). The active site of this enzyme contains a Mn_2 core. RNRs are involved in DNA biosynthesis. We have previously investigated one of the Mn^{II}_2 complexes described below as a class Ib Mn_2 RNR model.[19] One of the goals of this research was to synthesise further synthetic structural mimics of the class Ib Mn^{II}_2 RNRs active site.

To the best of our knowledge Mn_2 and Cu_2 complexes supported by the same ligand framework have not been investigated for comparison of their catecholase activity. We wanted to investigate their catecholase activity under nearly identical experimental conditions to compare their catalytic efficiency and to understand the role of the central metal ion. We herein report the synthesis of six dinuclear complexes (Figure 1), their full characterisation, and their aerobic catecholase reactivity (Scheme 1).

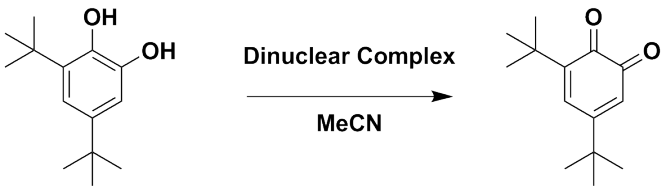

Scheme 1. Oxidation of 3,5-DTBC by Mn^{II}_2 and Cu^{II}_2 complexes.

Results and Discussion

Synthesis and characterisation of Mn^{II}_2 and Cu^{II}_2 complexes 1-6: The di-nucleating ligands N,N,N',N'-tetrakis(2-benzimidazolylmethyl)-2-hydroxo-1,3-diaminopropane (HPTB) and N,N,N',N'-tetrakis(2-(1-ethylbenzimidazolyl))-2-hydroxy-

School of Chemistry, Trinity College Dublin, The University of Dublin, College Green, Dublin 2, Ireland. E-mail: aidan.mcdonald@tcd.ie

Electronic Supplementary Information (ESI) available: [details of any supplementary information available should be included here]. See DOI: 10.1039/x0xx00000x

1,3-diaminopropane (N-Et-HPTB) were synthesised as previously described (see experimental section and supporting information for details).[20] $[Mn_2(O_2CR)(X\text{-}HPTB)](ClO_4)_2$ (where X = N-C_2H_5: R = CH_3 (**1**), C_6H_5 (**2**); and X = H: R = CH_3 (**3**), R = C_6H_5 (**4**)) (Figure 1) were synthesised using slight modifications of the procedure reported for the preparation of $[Mn_2(O_2CCH_3)(HPTB)](ClO_4)_2$ (**3**).[21] $[Cu_2(O_2CR)(HPTB)](ClO_4)_2$ (where R = CH_3 (**5**), C_6H_5 (**6**)) were synthesised using a procedure reported by Reed and co-workers for the preparation of $[Cu_2(O_2CCH_3)(N\text{-}Et\text{-}HPTB)](ClO_4)_2$.[20, 22] All complexes were obtained in reasonably good yields (**1**, 87%; **2**, 86%; **3**, 57%; **4**, 56%; **5**, 43%; **6**, 45%).

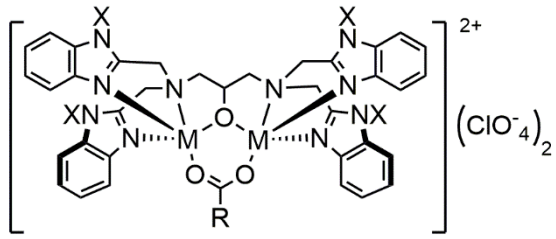

M = Mn; X = C_2H_5; R = CH_3 (**1**), C_6H_5 (**2**)
M = Mn; X = H; R = CH_3 (**3**), C_6H_5 (**4**)
M = Cu; X = H; R = CH_3 (**5**), C_6H_5 (**6**)

Figure 1. Structure of Mn^{II}_2 and Cu^{II}_2 complexes **1**-**6**.

Matrix assisted laser desorption/ionisation time of flight (MALDI-ToF) mass spectrometry analysis of complexes **1** and **2** showed prominent mass peaks attributable to the mono-cations $\{[Mn_2(O_2CR)(N\text{-}Et\text{-}HPTB)](ClO_4)\}^+$ (where R = CH_3 (**1**), C_6H_5 (**2**), Figures S1-2).[19] Electrospray ionisation mass spectrometry (ESI-MS) analysis of complexes **3** and **4** displayed mass peaks that correlate with the di-cations $[Mn_2(O_2CR)(HPTB)]^{2+}$ (R = CH_3 (**3**), R = C_6H_5 (**4**), Figures S3-S4). ESI-MS analysis of **5** and **6** also exhibited mass peaks corresponding to the monocations $\{[Cu_2(O_2CR)(HPTB)](ClO_4)\}^+$ (R = CH_3 (**5**), C_6H_5 (**6**), Figures S5-S6). ^{1}H nuclear magnetic resonance (NMR) analysis of complexes **1**-**4** yielded featureless spectra, presumably due to the broadening effect caused by the paramagnetic Mn^{II} ions. ^{1}H NMR analysis for complexes **5** and **6** matched those previously reported (Figures S7-S8).[22] Finally, elemental combustion analysis confirmed the elemental composition for complexes **1**-**6** (see experimental section).

A comparison of the attenuated total reflectance Fourier transform infrared (ATR-FTIR) spectra of complexes **1**-**6** (Figures S9-S11, Table 1) showed that they all displayed very similar vibrational properties. The $\nu_{C=O}$ values obtained for the asymmetric (1540-1560 cm^{-1}) and symmetric (1410-1450 cm^{-1}) stretches in complexes **1**-**6** agree well with those previously reported for complex **3** as well as other Cu^{II}_2 complexes bearing carboxylate bridges.[21, 23] Furthermore, the difference between the asymmetric and symmetric stretches (Δ, Table 1) for each complex was in the range expected for a bridging monodentate carboxylate ligand.[24, 25] Previously reported carboxylate-bridged Mn^{II}_2 complexes $[Mn_2(O_2CPh)_2(BPMP)](ClO_4)$ (HBPMP = 2,6-bis[bis(2-pyridylmethyl)aminomethyl]-4-methylphenol) displayed features at $\nu_{C=O}$ = 1570 cm^{-1} and 1400 cm^{-1},[26] while analogous Cu^{II}_2 complexes $[Cu_2(OAc)(P2\text{-}O)](ClO_4)_2$ and $[Cu_2(P2'\text{-}O)(OAc)(H_2O)](ClO_4)_2$, (P2-OH = N,N′,N″,N‴-tetrakis(2-pyridylethyl)-1,3-diamino-2-propanol, OAc = O_2CCH_3), exhibited $\nu_{C=O}$ = 1560 and 1460 cm^{-1}.[23] All six complexes displayed a strong stretch at ν = 1080 cm^{-1} corresponding to free ClO_4^- anion (Figures S9-11). Unfortunately, the ν_{asym}(Mn–O–Mn) stretch, expected around 720-750 cm^{-1},[27] could not be assigned in complexes **1**-**4** due to a strong ligand-based feature that was present (730-760 cm^{-1}, Figures S12-13 for ligand spectra). Overall, the vibrational properties of complexes **1**-**6** compared well to analogous complexes previously reported in the literature and indicated that an anionic carboxylate ligand bridged the metal centres.

	1[19]	**2**	**3**[this work]	**3**[21]	**4**	**5**	**6**
$^{asym}\nu_{C=O}$	1560	1547	1540	1564	1549	1560	1541
$^{sym}\nu_{C=O}$	1447	1450	1412	1428	1450	1451	1448
Δ	113	97	128	136	99	109	93

Table 1. Comparison of carboxylate ν_{asym} and ν_{sym} in dinuclear complexes **1**-**6** (all values in cm^{-1}).

Complexes **2**, **4**, **5**, and **6** were recrystallized from acetonitrile by diethylether (Et_2O) vapour diffusion to yield crystals suitable for X-ray diffraction measurements (Table S2, Figure 2). We previously reported the structure of **1**,[19] while the structure of **3** has been described elsewhere.[21] Each complex was found to consist of two five-coordinate metal atoms in either a square pyramidal or a distorted trigonal-bipyramidal geometry (Figure 2). The geometry at each metal centre was determined by the calculation of the corresponding τ_5 value.[28] This allowed us to determine if the metal site had more trigonal bipyramidal or square pyramidal character.

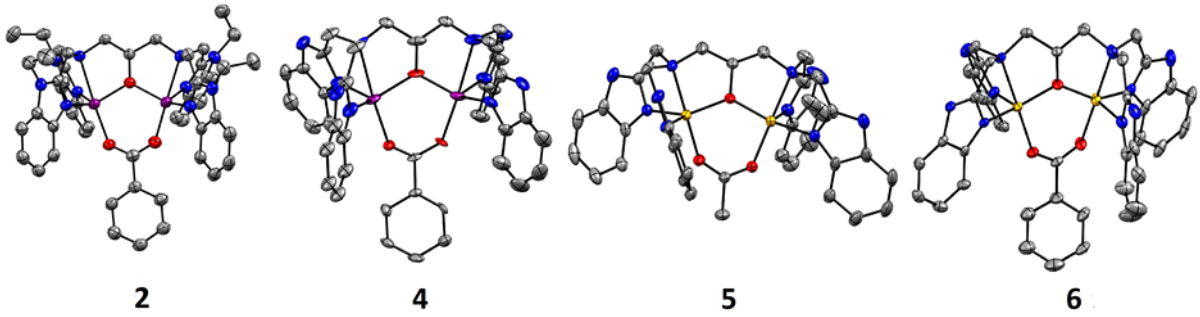

Figure 2. Thermal ellipsoid plots of complexes **2**, **4**, **5**, and **6** (from left to right). Hydrogen atoms and counter anions have been removed for clarity (purple = Mn, yellow = Cu, grey = C, blue = N, red = O). Ellipsoids are shown at 50% probability level.

A τ_5 value of 0 corresponds to a perfect square pyramidal geometry, while a τ_5 value of 1 indicates a perfect trigonal bipyramidal geometry.[28] Intermediary values indicated that the metal centre had a distorted structure, in between the two extremes. The Mn centres in complexes **1**, **2**, and **4** were in an almost perfect trigonal bipyramidal geometry (Table 2), while for complex **5**, one of the Cu centres was best described as distorted square pyramidal. The axial position of this square pyramid was capped by a long Cu-N_{benz} bond. This increased bond length was likely due to Jahn-Teller distortion of the square pyramid. For the other Cu centre in **5** and one of the Cu centres of complex **6**, the τ_5 value was ~0.5, while the second Cu centre in complex **6** had a τ_5 value of 0.7, a distorted trigonal bipyramidal structure. In summary, the Mn ions in complexes **1**-**4** displayed trigonal bipyramidal geometry in all complexes, and the Cu ions in **5** and **6** tended to display more distorted structures (Figure 2, Table 2).

τ_5	**1**[19]	**2**	**4**	**5**	**6**
M(1)	0.81	1.03	0.96	0.34	0.51
M(2)	0.98	1.05	0.96	0.55	0.7

Table 2. τ_5 values of dinuclear complexes **1**, **2**, **4**, **5**, and **6** (M = Mn or Cu).

In the X-ray crystallography determined structures of **2**, **4**, **5**, and **6**, the O-atoms of the carboxylate ligand (acetate or benzoate) bridged the two metal atoms in an axial position, corroborating our ATR-IR results that indicated a bridging carboxylate was present. The alkoxide O-atom of the heptadentate (N-Et-)HPTB ligand coordinated to the two metal atoms in equatorial sites, while the remaining N-atoms of the HPTB ligand occupied equatorial (benzimidazole N) and axial (amine N) sites. These observations were consistent with the structures reported for **1**[19] and **3**[21] and other complexes supported by the HPTB family of ligands.[22, 29-32] However, in the previously described structure of **3**, a butanol ligand was bound to one of the Mn^{II} ions, making it hexacoordinate, while the second Mn ion was pentacoordinate. In contrast, in **1**-**2** and **4**-**6** all metal ions displayed coordination numbers of five, with no solvent bound.

We originally prepared Mn_2 complexes **1**-**4** as mimics of the active site of the Class Ib Mn_2 Ribonucleotide Reductases (RNRs). The Mn···Mn distance in the X-ray crystal structure reported for class Ib Mn_2 RNR from *E. coli* was 3.7 Å,[33] from *B. subtilis* was 3.9 Å,[34] while from *C. ammoniagenes* a 3.3 Å metal-metal distance[35] was determined. In both *E. coli* and *B. subtilis*, the Mn ions were determined to be in the +2 oxidation state, but in *C. ammoniagenes* in the +3 oxidation state. The metal-metal separation for all four Mn_2 complexes **1**-**4** were very similar to each other (Table 3: 3.6, 3.5, 3.54, 3.55 Å, respectively). The Mn···Mn distances were slightly larger in the

	Model Complex								**Class Ib Mn_2-RNRs**					
	1[19]		**2**		**3**[21]		**4**		***E. coli* (Mn^{II}_2)**		***B. subtilis* (Mn^{II}_2)**		***C. ammoniagenes* (Mn^{III}_2)**	
	Mn1	Mn2	Mn1	Mn2	Mn1	Mn2	Mn1	Mn2	Mn1	Mn2	Mn1	Mn2	Mn1	Mn2
Coordination Number	5	5	5	5	5	6	5	5	6	6	6	5	6	5
Mn···Mn (Å)	3.6		3.5		3.54		3.55		3.7		3.9		3.3	

Table 3. Comparison of structural properties of complexes **1**-**4** and class Ib Mn_2 RNR active sites.

Mn^{II}_2 enzymatic active sites than in complexes **1**-**4**. The coordination number in the class Ib Mn_2 RNR active sites were either 5- or 6-coordinate, with a vacant site often postulated as the site of O_2-activation. The coordination numbers in **1**-**4** were five. Overall complexes **1**-**4** are thus reasonably reliable structural mimics for class Ib Mn_2 RNRs (Table 3).

The average Mn-N_{amine} and Mn-N_{benz} bond lengths of complex **2** were very close in values when compared to that of previously reported complex **1**.[19] Likewise, the average Mn-N_{amine} and Mn-N_{benz} bond lengths of complex **4** were very close in values when compared to that of previously reported complex **3** (Table S1). This was expected as complexes **1** and **2** were supported by the same ligand (N-Et-HPTB) while complexes **3**[21] and **4** were supported by the HPTB ligand. Comparison of the average Mn-N_{amine} and Mn-N_{benz} bond lengths of the Mn complexes **1**/**2** to that of **3**/**4**, showed those of complexes **1**/**2** to be shorter (Table S1). This was most likely due to the higher basicity of the alkylated ligand (N-Et-HPTB) versus the unalkylated HPTB ligand. Finally, a comparison of average metal-N_{amine} and metal-N_{benz} bond lengths of Cu complexes **5**/**6** to that of Mn complexes **1**-**4** showed those of complexes **5**/**6** to be shorter (Table S1). This can be attributed to a slightly larger atomic radius of the Mn atoms in **1**-**4** compared to the Cu atoms in **5** and **6**.

Apart from differences in Mn–N/O bond lengths in complexes **1**-**6**, we also noticed some structural differences between the acetate (**1**) and benzoate (**2**) bridged complexes. By over-laying the crystal structures of complexes **1** with **2** a noticeable difference in the positioning of the benzimidazole groups was observed depending on whether an acetate or benzoate bridge was present (Figure 3). This was evident as an apparent closing of the benzimidazole 'wings' in the acetate bridged complex **1** and an opening of the benzimidazole 'wings' in the benzoate bridged complex **2**. The closing of the benzimidazole 'wings' resulted in a slightly longer Mn···Mn distance in complex **1** (3.6 Å) while the opening of the 'wings' resulted in shorter distances in **2** (3.5 Å). However, no such difference was observed in the other complexes **3**-**6** (Figure S14). We believe the opening of the wings can be attributed to the benzoate bridge causing steric repulsion with the benzimidazole 'wings', forcing the benzimidazoles to rotate slightly when benzoate was present.

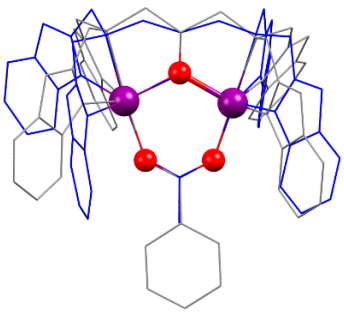

Figure 3. Overlapping structures of Mn^{II}_2 complexes **1** (blue wireframe) and **2** (grey wireframe) (ethyl groups have been removed for clarity).

The electrochemical properties of complexes **1**-**6** were studied by cyclic voltammetry (CV). The cyclic voltammograms of Mn_2 complexes **1**-**4** showed *quasi*-reversible peaks while those of the Cu^{II}_2 complexes **5**-**6** exhibited reversible reduction peaks (Figures S15-S20). The electrochemical data are summarised in Table 4.

Complex	$E_{1/2}$ (1) (V vs SCE)/ $E_{1/2}$ (2) (V vs SCE)	$(\Delta E)_{1,2}$ (V vs SCE) (=E_{red} (1) - E_{red} (2)[4]
1	0.70[a]	-
2	0.78[a]	-
3	-	-
4	0.77[a]	-
5	0.41/-0.47[b]	0.88
6	0.42/-0.41[b]	0.83

Table 4. Electrochemical data for dinuclear complexes **1**-**6** (a-Mn^{II}_2/Mn^{III}_2 redox couple, b-$Cu^{II}_2/Cu^{II}Cu^{I}$ and $Cu^{II}Cu^{I}/Cu^{I}_2$ redox couple).

The initial oxidation of Mn_2 complexes **1** at 0.7 V vs SCE, **2** at 0.78 V, and **4** at 0.77 V vs SCE was assigned to a two-electron process which was reversible. This was supported by the in-equivalence of the relative peak currents $I_{ox}/I_{red} \neq 1$ (1.46 for complex **1**, 1.8 for complex **2** and 1.7 for complex **4**) as well as a doubling of the peak potential difference with the scan rate between 50 and 100 mV/s.[37] Such two electron oxidation was previously observed for other Mn^{II}_2 complexes $[Mn_2(tmpdtne)Cl_2](ClO_4)_2.2DMF$ and $[Mn_2(tmpdtnb)Cl_2](ClO_4)_2.DMF.2H_2O$ (where tmpdtne = 1,2-bis[4,7-bis(2-pyridylmethyl)-1,4,7-triazacyclonon-1-yl]-ethane and tmpdtnb = 1,4-bis[4,7-bis(2-pyridylmethyl)-1,4,7-triazacyclonon-1-yl]-butane.[38] The two-electron oxidation process for complex **1** was followed by an irreversible one-electron oxidation process at 1.55 V vs SCE. The same was observed for complex **4** at 1.19 V vs SCE, however no second oxidation was observed for **2**. Pessiki and co-workers first reported the electrochemical data for complex **3** in 1994 where they found an initial two electron oxidation process (0.86 V) followed by a second oxidation (1.3 V) which was irreversible.[21] We did not observe the first oxidation of **3** using our instrumental set-up. We did observe one irreversible oxidation process of **3** at 1.38 V vs SCE.

For complexes **5** and **6**, an initial reversible reduction peak 0.41 V and 0.42 V vs SCE respectively was measured. In contrast, Cu^{II}_2 systems such as $[Cu_2(H_3bbppnol)(\mu\text{-}OAc)(H_2O)_2]Cl_2.2H_2O$ (H_3bbppnol = N,N`-bis(2-hydroxybenzyl)-N,N`-bis-(pyridylmethyl)]-2-hydroxy-1,3-propanediamine), $[Cu_2(H_2btppnol)(\mu\text{-}OAc)](ClO_4)_2$ (H_2btppnol = N-(2-hydroxybenzyl)-N,N`,N`-tris(2-pyridylmethyl)]-1,3-diaminopropan-2-ol) and $[Cu_2(P1\text{-}O)(OAc)](ClO_4)_2$ (P1-O = 1,3-bis[(2-pyridylmethyl)amino]-propanolate) showed irreversible reductions.[4] Furthermore Cu^{II}_2 complexes supported by Schiff-base ligands ($[Cu_2(H_2L2^2)(OH)(H_2O)(NO_3)](NO_3)_3.2H_2O$ ($L2^2$ =

2,6-bis(N-ethylpiperazine-iminomethyl)-4methyl-phenolato) and $[Cu_2(L2^3)(OH)(H_2O)_2](NO_3)_2$ ($L2^3$ = 2,6-bis(N-ethylpyrrolidine-iminomethyl)-4methyl-phenolato)) also exhibited an irreversible redox couple.[5] Thus the electrochemical behaviour of the biomimetic complexes could provide further insight into the catecholase reaction mechanism.

Catechol oxidase reactivity: The catalytic oxidation of catechol by complexes **1**-**6** was examined in acetonitrile solutions, under aerobic conditions using 3,5-di-*tert*-butylcatechol (3,5-DTBC) as a biomimetic catechol substrate. 3,5-DTBC was used as a substrate as it had a low redox potential and its oxidised quinone form, 3,5-di-*tert*-butylquinone (3,5-DTBQ), was easily identified using electronic absorption spectroscopy.[5, 18] Moreover 3,5-DTBC has bulky substituents that prevent other side-reactions such as oxidative ring opening. The oxidation product 3,5-DTBQ exhibited an absorption band at λ_{max} = 400 nm (ε = 1900 $M^{-1}cm^{-1}$, Figure 4).[39] For complexes **1**-**6** we observed the catalytic formation of 3,5-DTBQ from 3,5-DTBC (Figures 4 and S21-25).

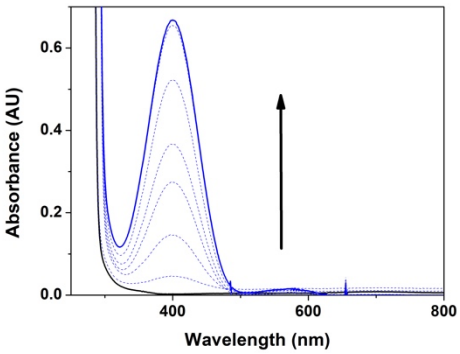

Figure 4. Electronic absorption spectral changes showing formation of 3,5-DTBQ (solid blue trace) after addition of 3,5-DTBC (25 equivalents) to complex **2** (0.1 mM, black trace) in acetonitrile at 25 °C.

*Complexes **5**-**6**:* Cu^{II}_2 complexes have previously been demonstrated to be excellent catechol oxidase mimics, we therefore explored the reactivity of **5** and **6** first.[4-10] A plot of quinone produced (λ_{max} = 400 nm) versus time displayed a biphasic kinetic behaviour (Figure 5) for both complexes. The initial phase represented approximately 0.5 turnovers of the catalyst, while the latter phase showed a further 1.5 turnovers. The catalyst generally turned over at least 10 times prior to the reaction being quenched. Such biphasic kinetic behaviour has been previously observed by Monzani *et al.*[6, 7] for Cu^{II}_2-mediated catechol oxidation where three Cu^{II}_2 complexes supported by *m*-xylyl tetrabenzimidazole showed a fast initial phase followed by a slower phase of the reaction.[6, 7] Other Cu^{II} systems investigated in catecholase activity showed no biphasic behaviour.[40] For Cu^{II}_2 complexes **5** and **6** the biphasic behaviour was typified by an initial fast phase and a slower second reaction phase. The initial phase was about 10-fold faster than the second phase for both complexes (Figure S26). Additionally, we observed that the rate of the first phase was dependent on the concentration of 3,5-DTBC while the second phase rate was independent of the substrate concentration (Figure S26).

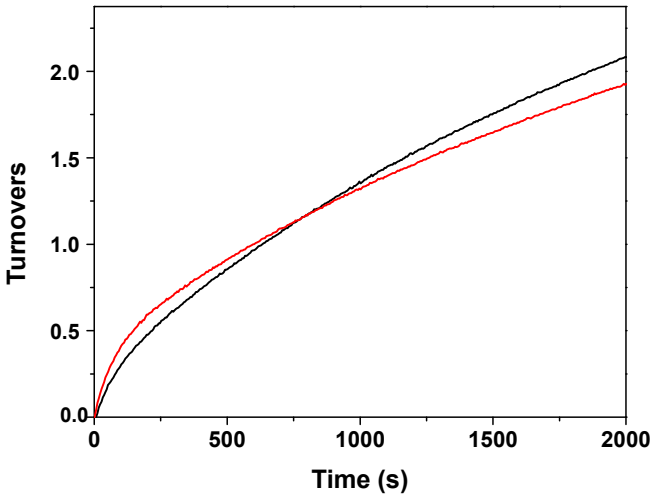

Figure 5. Plot of total turnovers (mol product/mol catalyst) versus time for the reaction of complexes **5** (black trace) and **6** (red trace) with 50 equivalents 3,5-DTBC in acetonitrile.

The measured kinetic results for the first phase of the reaction were consistent with Michaelis-Menten behaviour, and correlated well with previous observations.[4, 5, 8, 40] A Michaelis-Menten treatment was performed and Lineweaver-Burk analyses were used to determine the binding constant (K_M), maximum velocity (V_{max}), and the turnover number (k_{cat}, Figure 6, Table 5).[9, 18] The V_{max} values for **5** and **6** were almost the same. However, the K_M parameter, which reflects the substrate's dissociation constant, was four times higher for complex **5** than complex **6**. This implied a relatively weak binding of the catechol (3,5-DTBC), meaning the catechol could more easily dissociate from the Cu^{II}_2 core in **5**. The slightly lower V_{max} of **6** could be attributed to the increased steric bulk of the benzoate carboxylate bridge in complex **6** (0.020 Ms^{-1}) when compared to the acetate bridge in complex **5** (0.024 Ms^{-1}). This also resulted in a slightly lower k_{cat} value for complex **6** (44 h^{-1}) when compared to complex **5** (48 h^{-1}). Therefore, based on the kinetic parameters, the Cu^{II}_2 complex **6** proved to have a slighter higher catalytic efficiency than the Cu^{II}_2 complex **5**.

Figure 6. Plots of the first order reaction rate against [3,5-DTBC] obtained for the reaction between 3,5-DTBC and **5** (i) or **6** (ii) (first phase of the reactions); and Lineweaver-Burk plots for the same reactions for **5** (iii) and **6** (iv)**.**

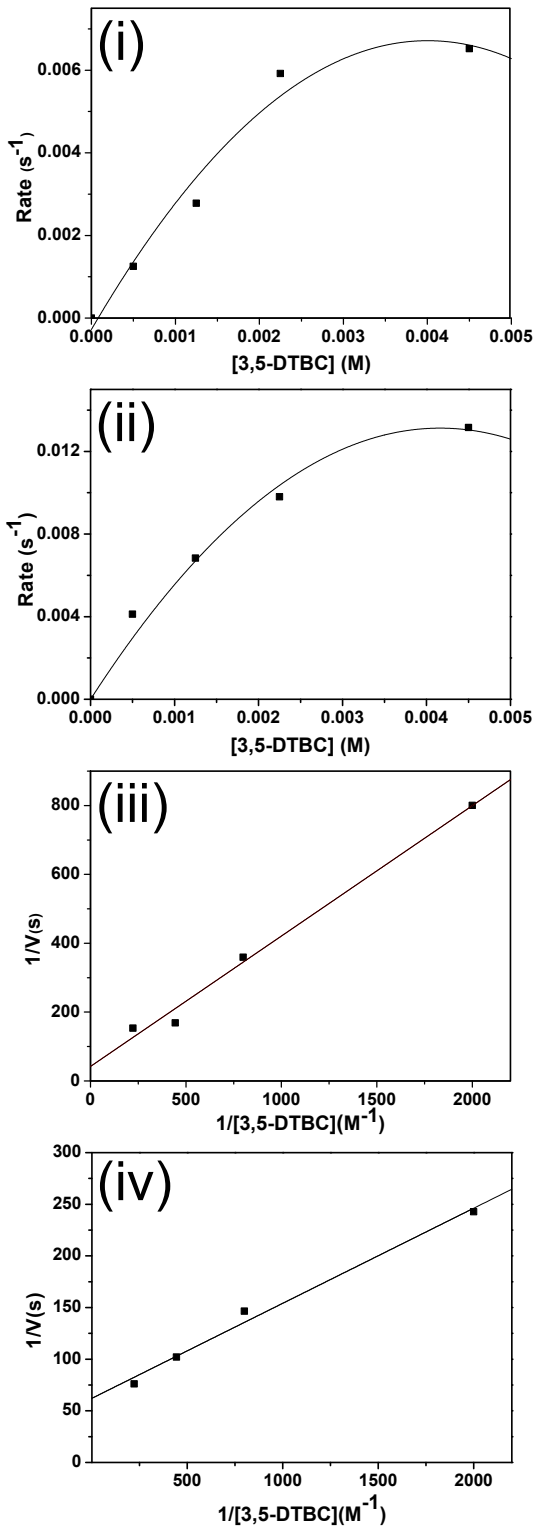

We were interested in comparing the catecholase reactivity of Cu^{II}_2 complexes **5**-**6** to that of Mn^{II}_2 complexes **1**-**4** supported by the same ligands. We explored the catecholase reactivity of **1**-**4** using 3,5-DTBC as a substrate under the same conditions outlined for **5** and **6** above. In contrast to complexes **5** and **6**, complexes **1**, **2**, and **4** displayed a kinetic trace that appeared to display non-linear multi-phasic behaviour (Figures 7, S27-31). The kinetic trace was made up of a slow initiation phase, followed by a faster hyperbolic phase and a subsequent slower phase again. In contrast, the oxidation of 3,5-DTBC by **3** exhibited an almost linear behaviour (Figure S29). For **1**, **2**, and **4**, we surmise that the initial reaction phase was possibly attributed to the oxidation of the Mn^{II}_2 complexes to a higher oxidation state by atmospheric O_2. The subsequent reaction phases are presumably analogous to the biphasic reactivity observed for **5** and **6**. The (estimated) rate constants estimated for the first and third phase of the reaction were independent of substrate concentration (Table S3). The rate of the second phase of the reaction was substrate concentration dependent. However, at higher substrate concentrations, the rate of the second phase of the reaction reached a saturation point (Figure S32).

Unfortunately, it was not possible to accurately ascertain when one phase finished, and the next phase started. Therefore, the accuracy of any kinetic measurement would be very low, and it is not possible to explore if Michaelis-Menten kinetics were obeyed. We were able to determine the k_{cat} values for the reaction of complexes **1**-**4** with 3,5-DTBC (Table 5). Complex **1** had a higher k_{cat} value (44 h^{-1}) than complex **2** (24 h^{-1}), both being supported by the alkylated HPTB ligand, and the change in rate seemingly caused by the change from acetate (**1**) to benzoate (**2**) bridging ligand. Complexes **3** and **4** supported by the non-alkylated HPTB ligand resulted in the same k_{cat} value (8 h^{-1}). The dramatic drop-off in k_{cat} for the complexes supported by the unalkylated HPTB ligand (8 h^{-1} versus 44 h^{-1}) suggested that the Mn^{II}_2 core prefers to be electron-rich for efficient catecholase reactivity. Thus, based only on the k_{cat} values, the Mn^{II}_2 complex **1** supported by the more electron rich N-Et-HPTB and smaller bridging acetate ligands proved to display the highest overall reaction rate in the series of Mn^{II}_2 complexes **1**-**4**.

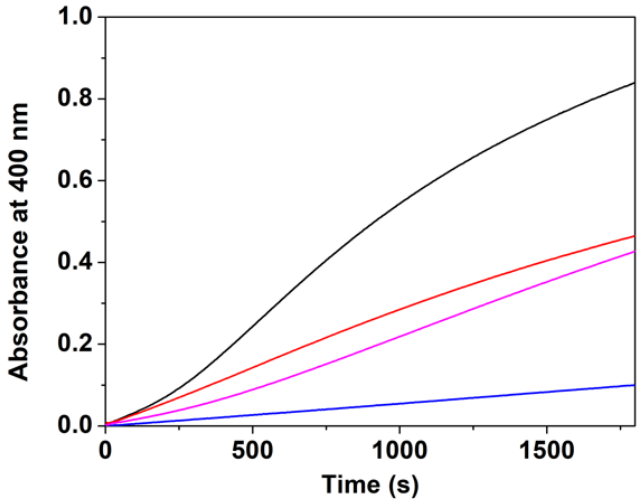

Figure 7. Plot of absorbance at λ_{max} = 400 nm versus time for the reaction between 25 equivalents 3,5-DTBC and Mn^{II}_2 complexes **1** (black trace), **2** (red trace), **3** (blue trace), and **4** (pink trace), in acetonitrile at 25 °C.

While the catechol oxidase reactivity of a series of mononuclear Mn^{III} complexes has been widely investigated,[11, 13, 18] Mn^{II}_2 complexes have been less explored in catecholase oxidase reactivity.[41] Mn^{III} complexes showed a high catalytic efficiency with k_{cat} = 270-336 h^{-1}.[11, 42] For a Mn^{II}_2 complex supported by a binucleating ligand (1,4-di(2'-pyridyl)aminophthalazine) a k_{cat} of 167 h^{-1} was obtained.[41] This value was comparable to the values reported for mononuclear Mn^{III} complexes[13, 42] but higher than the k_{cat} obtained for Mn^{II}_2 complexes **1**-**4** (Table 5). Furthermore, Ray and co-workers probed the catecholase activity of a mixed valent $Mn^{III}_2Mn^{II}$ complex in the catalytic oxidation of 3,5-DTBC which showed a k_{cat} = 644 h^{-1}.[17] Thus, the Mn^{II}_2 complexes **1**-**4** exhibited moderate catecholase activity when compared to previously reported complexes, indicating that catalysts in the higher Mn^{III} oxidation state are likely to be more reactive.

We were unable to find a correlation between the catalytic rate constants and the individual redox potentials or $(\Delta E)_{1,2}$ of Mn^{II}_2 complexes **1**-**4** or of Cu^{II}_2 complexes **5** and **6**. Similarly, Krebs *et al.* failed to establish any relationship between the electrochemical properties of their Cu^{II}_2 complexes and the oxidation potential of 3,5-di-*tert*-butylcatechol (3,5-DTBC), the substrate used.[39, 43-45] The same observation was reported by Das and co-workers in 2014.[9] In contrast, Neves *et. al* found a good correlation between the kinetic parameter k_2 (= k_{cat}/K_M) and $(\Delta E)_{1,2}$ (= $E(red)_1$-$E(red)_2$) in their Cu^{II}_2 complexes.[4] However they could not establish any correlation between k_{cat}/K_M and the individual redox potentials of the complexes ($E(red)_1$ and $E(red)_2$).

Complex	Turnover number (k_{cat}, h^{-1})	V_{max} (M s^{-1})	K_M	k_{cat}/K_M (M^{-1} h^{-1})
1	44	-	-	-
2	24	-	-	-
3	8	-	-	-
4	8	-	-	-
5	48	0.024	$8.98*10^{-3}$	5345
6	44	0.02	$1.8*10^{-3}$	24444

Table 5. Kinetic parameters for the oxidation of 3,5-DTBC by complexes **1**-**6**.

In the series **1**-**6** (Table 5), we noticed that Cu^{II}_2 complexes **5** and **6** had the highest k_{cat} values, whereas Mn^{II}_2 complex **1**-**4** displayed lower k_{cat} values (apart from **1**). We surmise the lower activity of the Mn^{II}_2 complexes can be attributed to the (slow) initiation phase in their reaction with 3,5-DTBC. This initiation phase is presumably the oxidation of the Mn^{II}_2 precursor to a higher oxidation state to facilitate catechol oxidation through electron transfer. This postulate is supported by observations previously made on Mn^{III} and Mn^{II} catechol oxidants, where the Mn^{III} catalysts generally displayed higher reaction rates.[11, 13, 17, 18, 41, 42] A trend could be observed where the acetate bridged carboxylate complexes (**1** and **5**) had higher k_{cat} values than the corresponding benzoate bridged complexes (**2** and **6**). Also, complexes supported by the un-alkylated ligand (complexes **3** and **4**) had a lower turnover number when compared to complexes supported by the alkylated ligand (complexes **1** and **2**). Overall, in this series of dinuclear complexes the Cu^{II}_2 complexes **5** and **6** proved to be somewhat more reactive catalysts for the catechol oxidase reaction of 3,5-DTBC when compared to the Mn^{II}_2 complexes **1**-**4**.

Catalyst	Turnover frequency (k_{cat}, s^{-1})	k_{cat}/K_M ($M^{-1}s^{-1}$)	Ref.
1	0.012	-	this work
2	0.007	-	this work
3	0.002	-	this work
4	0.002	-	this work
$[Mn(bpia)(OAc)(OCH_3)](PF_6)$	0.024	16	13
$[Mn(bipa)(OAc)(OCH_3)](PF_6)$	0.028	23	13
$[MnL^1Cl].2H_2O$	0.5	710	18
$[MnL^4Cl].4H_2O$	5	602	18
5	0.013	1.45	this work
6	0.012	6.7	this work
$[Cu_2(H_2bbppnol)(\mu\text{-}OAc)(H_2O)_2]Cl_2.2H_2O$	0.0079	10	4
$[Cu_2(Hbtppnol)(\mu\text{-}OAc)](ClO_4)_2$	0.0078	8.1	4
$[Cu_2(LB5)](ClO_4)_4$	0.31	590	6
$[Cu_2(L\text{-}55)](ClO_4)_4$	1.40	900	6
$[Cu_2(EBA)](PF_6)_4$	0.7	60	7
$[Cu_2(L_2^3)(OH)(H_2O)](NO_3)_2$	4	526	5

Table 6. Comparison of kinetic parameters (k_{cat} and k_{cat}/K_M) of complexes **1**-**6** to previously reported Mn and Cu complexes. (Bpia = bis-(picolyl)(N-methylimidazole-2-yl)amine; Bipa = bis(N-methylimidazole-2-yl)(picolyl)amine; L^1 = N, N'-ethylenebis(3-formyl-5-methyl-salicylaldimine); L^4 = N, N'-cyclohexenebis(3-formyl-5-methylsalicylaldimine); H_2bbppnol = N, N'-bis(2-hydroxybenzyl)-N,N'-bis-(pyridylmethyl)-2-hydroxy-1,3-propanediamine; Hbtppnol = N-(2-hydroxybenzyl)-N,N',N''-tris(2-pyrisylmethyl)-1,3-diaminopropan-2-ol; LB5 = N,N,N',N',N''-pentakis[(1-methyl-2-benzimidazolyl)methyl]dipropylenetriamine; L-55 = α,α'-bis{bis[(1-methyl-2-bezimidazolyl)methyl]amino}-*m*-xylene; EBA = 1,6-bis[[bis(1-methyl-2-benzimidazolyl)methyl]amino]-*n*-hexane; L_2^3 = 2,6-bis(N-ethylpyrrolidine-iminomethyl)-4-methyl-phenolato).

The turnover frequency of Mn^{II}_2 complexes **1**-**4** are slightly lower than those obtained for mononuclear Mn^{III} complexes supported by tetradentate tripodal ligands (Table 6). Likewise, mononuclear Mn^{II} complexes exhibited higher turnover numbers than the dinuclear Mn^{II}_2 complexes reported here.

Furthermore, the Cu^{II}_2 complexes **5** and **6** exhibited comparable turnover frequencies to the Cu^{II}_2 complexes supported by the H_2bbppnol and Hbtppnol ligands (Table 6) but a lower k_{cat}/K_M value than these complexes. Moreover, the Cu^{II}_2 complexes bearing the LB5, L-55, EBA, and L_2[3] ligands displayed higher turnover numbers and a better catalytic efficiency that the Cu^{II}_2 complexes described here. It must be noted, however, that these catalytic reactions were not all performed under the same conditions (solvent, temperature etc.), and therefore not all comparisons are fair. Overall, The family of complexes fits well within comparable Mn and Cu catalysts previously reported, allowing for an accurate comparison of the effect of substituting Mn for Cu in catcholase mimics to understand the role of the metal ion.

Conclusions

We have reported the synthesis and characterisation of a family of Mn^{II}_2 and Cu^{II}_2 complexes supported by the same dinucleating ligands. These complexes were structurally characterised using X-ray crystallography, demonstrating the Mn^{II}_2 complexes to be reliable mimics of the active site of class Ib Mn_2 RNRs. Four Mn^{II}_2 (**1**-**4**) and two Cu^{II}_2 (**5**-**6**) complexes were investigated as catechol oxidase mimics. All six dinuclear complexes were found to be effective catalysts for aerobic catechol oxidation. The k_{cat} values for all six complexes were calculated and our analysis revealed that Cu^{II}_2 complexes **5** and **6** were slightly more efficient catalysts when compared to Mn^{II}_2 complexes **1**-**4** supported by the same ligand framework. Furthermore, complexes support by the more electron-rich N-Et-HPTB ligand displayed higher activity. These results suggest that for more efficient catecholase activity, relatively electron rich late transition metals (Cu) and strong donor ligands are ideal.

Experimental

Materials

All reactions with air sensitive materials were conducted in a glove box under an N_2 atmosphere. All reagents and solvents were purchased from commercial sources. Anhydrous N,N-dimethylformamide was purchased and used without further purification. Anhydrous tetrahydrofuran, acetonitrile, and diethyl ether were dispensed through an Innovative Technology PureSolvEN solvent purification system and de-oxygenated by purging with Ar. N,N,N',N'-tetrakis(2-benzimidazolylmethyl)-2-hydroxo-1,3-diaminopropane (HPTB) and N,N,N',N'-tetrakis(2-(1-ethylbenzimidazolyl))-2-hydroxy-1,3-diaminopropane (N-Et-HPTB) were synthesised as previously described.[46] Complex **1** was synthesised as previously described.[19] Complex **3** ($[Mn_2(O_2CCH_3)(HPTB)](ClO_4)_2$) was synthesised using a modification of a procedure reported by Dismukes and co-workers,[21] (here complex **3** was recrystallized from acetonitrile/diethyl ether).

Instrumentation

^{1}H NMR analysis was performed on a Bruker Avance III 400 MHz instrument. Electrospray ionisation (ESI) mass spectra were obtained using a Micromass time of flight spectrometer. Matrix assisted laser desorption ionisation (MALDI) mass spectra were acquired using a Maldi QTOF Premier MS System. Infra-red spectra were recorded using a Perkin-Elmer Spectrum FT-IR spectrometer. Electronic absorption spectra were recorded in quartz cuvettes on a Hewlett Packard (Agilent) 8453 diode array spectrophotometer (190-1100 nm range) coupled to a liquid nitrogen cooled cryostat from Unisoku Scientific Instruments (Osaka, Japan). X-ray crystallography was performed on a Bruker APEX Kappa Duo system at 100 K using an Oxford Cobra cryosystem. Cyclic voltammetry (CV) experiments were conducted with a CH Instruments 600E electrochemical analyser, using a glassy carbon working electrode, a platinum wire counter electrode and a $AgNO_3$ reference electrode.

Synthesis

Synthesis of $[Mn_2(O_2CC_6H_5)(N\text{-}Et\text{-}HPTB)](ClO_4)_2$ (2)

N-Et-HPTB (0.18 g, 0.25 mmol), benzoic acid (1.11 mmol), and sodium benzoate (0.12 g, 0.81 mmol) were combined in a premixed 3:1 ethanol-water solution (70 mL). After stirring for 15 min, $Mn^{II}(OAc)_2.4H_2O$ (0.11 g, 0.45 mmol) dissolved in ethanol (10 mL) was added. The mixture was allowed to stir for 30 min, after which time $NaClO_4$ (0.39 g, 3.19 mmol) was added as an ethanol/water solution (10 mL). The reaction mixture was allowed to stir for 2 h and then it was allowed to stand at 0 °C overnight. A pink/white crystalline precipitate formed that was collected by filtration. Re-crystallisation from CH_3CN/Et_2O yielded crystals suitable for X-ray diffraction analysis.

Yield: 0.25 g, 86%. Anal. Calcd (found) for $C_{50}H_{54}Cl_2Mn_2N_{10}O_{11}.H_2O$: C, 51.34 (51.23); H, 4.83 (4.44); N, 11.97 (11.83). ν_{max} (ATR-FTIR)/cm^{-1}: μ_2-carboxylate 1596 (asymmetric) and 1493 (symmetric). Maldi-Tof MS (*m/z*): Found 1051.2595 ($[M\text{-}ClO_4^-]^+$. $C_{50}H_{54}ClMn_2N_{10}O_7^+$ Requires 1051.2632).

$[Mn_2(O_2CCH_3)(HPTB)](ClO_4)_2$ (3)

Complex **3** was synthesised according to a previously reported procedure on half the scale.[21] While the previously reported complex **3** was recrystallized from dichloromethane/chloroform/butanol,[21] we recrystallized complex **3** from acetonitrile/ diethyl ether. The ligand HPTB (0.12 g, 0.2 mmol), acetic acid (0.02 g, 0.33 mmol), and sodium acetate (0.09 g, 0.66 mmol) were combined in 34 mL of a premixed 3:1 ethanol/water solution. After stirring for 15 mins, $Mn^{II}(OAc)_2.4H_2O$ (0.08 g, 0.33 mmol) dissolved in 5 mL of ethanol was added. The mixture was allowed to stir for 30 mins at room temperature after which time $NaClO_4$ (0.4 g, 2.7 mmol) was added as a 1:1 ethanol/water solution. The reaction mixture was allowed to stir for 1 h after which the volume was

reduced under vacuum and placed in a fridge overnight. A white powder was obtained that was filtered.

Yield: 0.1 g, 57%. ν_{max} (ATR-FTIR)/cm^{-1}: μ_2-carboxylate 1540 (asymmetric) and 1412 (symmetric). Maldi-Tof MS (*m/z*): Found 389.0936 ($[M-(ClO_4^-)_2]^{2+}$. $C_{42}H_{38}Mn_2N_{10}O_3^{2+}$ Requires 389.0866).

$[Mn_2(O_2CC_6H_5)(HPTB)](ClO_4)_2$ (4)

The ligand HPTB (0.25 g, 0.41 mmol), benzoic acid (0.2 g, 1.65 mmol), and sodium benzoate (0.19 g, 1.3 mmol) were combined in 70 mL of a premixed 3:1 ethanol/water solution. After stirring for 15 mins, $Mn^{II}(OAc)_2.4H_2O$ (0.18 g, 0.73 mmol) dissolved in 10 mL of ethanol was added. The mixture was allowed to stir for 30 mins at room temperature after which time $NaClO_4$ (0.6 g, 4.95 mmol) was added as a 1:1 ethanol/water solution (10 mL). The reaction mixture was allowed to stir for 1 h after which the volume was reduced under vacuum and put in the fridge for 2 days. A white powder was obtained that was collected by filtration.

Yield: 0.16 g, 56%. Anal. Calcd (found) for $C_{42}H_{38}Cl_2Mn_2N_{10}O_{11}$: C, 48.52 (48.13); H, 3.68 (3.7); N, 13.47 (13.07). ν_{max} (ATR-FTIR)/cm^{-1}: μ_2-carboxylate 1549 (asymmetric) and 1450 (symmetric). Maldi-Tof MS (*m/z*): Found 420.1008 ($[M-(ClO_4^-)_2]^{2+}$. $C_{42}H_{38}Mn_2N_{10}O_3^{2+}$ Requires 420.0945).

General procedure for synthesis of complexes 5-6

HPTB (0.3 g, 0.49 mmol) and $Cu(ClO_4)_2.6H_2O$ (0.37 g, 0.98 mmol) were dissolved separately in ethanol (5 mL each). The two solutions were mixed and stirred together for 2 hours at room temperature. To the resulting blue solution NaO_2CX (X = CH_3, C_6H_5) (0.49 mmol) was added and the reaction was stirred overnight. A blue green precipitate formed that was collected by filtration. Recrystallisation from CH_3CN/Et_2O yielded crystals suitable for x-ray diffraction structural analysis of complexes **5** and **6**.

$[Cu_2(O_2CCH_3)(HPTB)](ClO_4)_2$ (5)

Yield: 0.22 g, 43%. Anal. Calcd (found) for $C_{37}H_{36}Cl_2Cu_2N_{10}O_{11}.H_2O$: C, 43.88 (43.53); H, 3.41 (3.41); N, 13.83 (13.42). ν_{max} (ATR-FTIR)/cm^{-1}: μ_2-carboxylate 1560 (asymmetric) and 1451 (symmetric). ESI-MS (*m/z*): Found 893.1071 ($[M-(ClO_4)]^{1+}$. $C_{37}H_{36}ClCu_2N_{10}O_7^+$ requires 893.1064).

$[Cu_2(O_2CPh)(HPTB)](ClO_4)_2$ (6)

Yield: 0.23 g, 45%. Anal. Calcd (found) for $C_{42}H_{38}Cl_2Cu_2N_{10}O_{11}.H_2O$: C, 46.93 (46.51); H, 3.75 (3.42); N, 13.03 (12.58). ν_{max} (ATR-FTIR)/cm^{-1}: μ_2-carboxylate 1541 (asymmetric) and 1448 (symmetric). ESI-MS (*m/z*): Found 955.1213 ($[M-(ClO_4)]^{1+}$. $C_{42}H_{38}ClCu_2N_{10}O_7^+$ Requires 955.1211).

Reactivity Studies

In quartz cuvettes, stirring solutions of complexes **1**-**6** (0.1 mM, 2 mL) in acetonitrile (CH_3CN) were treated with different concentrations ($5*10^{-4}$, $12.5*10^{-3}$, $2.25*10^{-3}$ or $4.5*10^{-3}$ M) of 3,5-di-*tert*-butylcatechol (3,5-DTBC) in CH_3CN, under aerobic conditions at 25 °C. The reaction was monitored by electronic absorption spectroscopy by following the formation of the oxidised product 3,5-di-*tert*-butylquinone (3,5-DTBQ) which exhibited an absorption band at λ_{max} = 400 nm (ε = 1900 $M^{-1}cm^{-1}$ in acetonitrile).[39]

Conflicts of interest

There are no conflicts to declare.

Acknowledgements

This publication has emanated from research supported by the Irish Research Council (IRC) under Grant Number GOIPG/2014/942 to A. Magherusan. Research in the McDonald lab is supported in part by the European Union (ERC-2015-STG-678202) and a research grant from Science Foundation Ireland (SFI/15/RS-URF/3307).

Notes and references

1. C. Gerdemann, C. Eicken and B. Krebs, *Acc. Chem. Res.*, 2002, **35**, 183-191.
2. S. Torelli, C. Belle, I. Gautier-Luneau, J. L. Pierre, E. Saint-Aman, J. M. Latour, L. Le Pape and D. Luneau, *Inorg. Chem.*, 2000, **39**, 3526-3536.
3. C. Belle, K. Selmeczi, S. Torelli and J.-L. Pierre, *C. R. Chim.*, 2007, **10**, 271-283.
4. A. Neves, L. M. Rossi, A. J. Bortoluzzi, B. Szpoganicz, C. Wiezbicki, E. Schwingel, W. Haase and S. Ostrovsky, *Inorg. Chem.*, 2002, **41**, 1788-1794.
5. K. S. Banu, T. Chattopadhyay, A. Banerjee, S. Bhattacharya, E. Suresh, M. Nethaji, E. Zangrando and D. Das, *Inorg. Chem.*, 2008, **47**, 7083-7093.
6. E. Monzani, L. Quinti, A. Perotti, L. Casella, M. Gullotti, L. Randaccio, S. Geremia, G. Nardin, P. Faleschini and G. Tabbì, *Inorg. Chem.*, 1998, **37**, 553-562.
7. E. Monzani, G. Battaini, A. Perotti, L. Casella, M. Gullotti, L. Santagostini, G. Nardin, L. Randaccio, S. Geremia, P. Zanello and G. Opromolla, *Inorg. Chem.*, 1999, **38**, 5359-5369.
8. S. Mandal, J. Mukherjee, F. Lloret and R. Mukherjee, *Inorg. Chem.*, 2012, **51**, 13148-13161.
9. P. Chakraborty, J. Adhikary, B. Ghosh, R. Sanyal, S. K. Chattopadhyay, A. Bauza, A. Frontera, E. Zangrando and D. Das, *Inorg. Chem.*, 2014, **53**, 8257-8269.
10. J. Reim and B. Krebs, *J. Chem. Soc., Dalton. Trans.*, 1997, 3793-3804.
11. A. Majumder, S. Goswami, S. R. Batten, M. Salah El Fallah, J. Ribas and S. Mitra, *Inorg. Chim. Acta.*, 2006, **359**, 2375-2382.
12. P. Kar, Y. Ida, T. Kanetomo, M. G. Drew, T. Ishida and A. Ghosh, *Dalton. Trans.*, 2015, **44**, 9795-9804.
13. M. U. Triller, D. Pursche, W. Y. Hsieh, V. L. Pecoraro, A. Rompel and B. Krebs, *Inorg. Chem.*, 2003, **42**, 6274-6283.
14. A. Jana, N. Aliaga-Alcalde, E. Ruiz and S. Mohanta, *Inorg. Chem.*, 2013, **52**, 7732-7746.
15. A. Guha, T. Chattopadhyay, N. D. Paul, M. Mukherjee, S. Goswami, T. K. Mondal, E. Zangrando and D. Das, *Inorg. Chem.*, 2012, **51**, 8750-8759.
16. J. Adhikary, P. Chakraborty, S. Das, T. Chattopadhyay, A. Bauza, S. K. Chattopadhyay, B. Ghosh, F. A. Mautner, A. Frontera and D. Das, *Inorg. Chem.*, 2013, **52**, 13442-13452.
17. K. Chattopadhyay, G. A. Craig, M. J. Heras Ojea, M. Pait, A. Kundu, J. Lee, M. Murrie, A. Frontera and D. Ray, *Inorg. Chem.*, 2017, **56**, 2639-2652.
18. K. S. Banu, T. Chattopadhyay, A. Banerjee, M. Mukherjee, S. Bhattacharya, G. K. Patra, E. Zangrando and D. Das, *Dalton. Trans.*, 2009, **40**, 8755-8764.
19. A. M. Magherusan, A. Zhou, E. R. Farquhar, M. Garcia-Melchor, B. Twamley, L. Que, Jr. and A. R. McDonald, *Angew. Chem. Int. Ed. Engl.*, 2018, **57**, 918-922.

20. V. McKee, M. Zvagulis, J. V. Dagdigian, M. G. Patch and C. A. Reed, *J. Am. Chem. Soc.*, 1984, **106**, 4765-4772.
21. P. J. Pessiki, S. V. Khangulov, D. M. Ho and G. C. Dismukes, *J. Am. Chem. Soc.*, 1994, **116**, 891-897.
22. J. M. Brink, R. A. Rose and R. C. Holz, *Inorg. Chem.*, 1996, **35**, 2878-2885.
23. G. S. Siluvai and N. N. Murthy, *Polyhedron*, 2009, **28**, 2149-2156.
24. R. R. Lynn, W. B. Tolman, S. J. Lippard, *New. J. Chem.* , 1991, **15**, 417-430.
25. G. Deacon, *Coord. Chem. Rev.*, 1980, **33**, 227-250.
26. M. Suzuki, M. Mikuriya, S. Murata, A. Uehara, H. Oshio, S. Kida and K. Saito, *Bull. Chem. Soc. Jpn.*, 1987, **60**, 4305-4312.
27. R. Hage, B. Krijnen, J. B. Warnaar, F. Hartl, D. J. Stufkens and T. L. Snoeck, *Inorg. Chem.*, 1995, **34**, 4973-4978.
28. A. W. Addison, T. N. Rao, J. Reedijk, J. van Rijn and G. C. Verschoor, *J. Chem. Soc., Dalton Trans.* , 1984, 1349-1356.
29. J. R. Frisch, V. V. Vu, M. Martinho, E. Munck and L. Que, Jr., *Inorg. Chem.*, 2009, **48**, 8325-8336.
30. A. L. Feig, M. T. Bautista and S. J. Lippard, *Inorg. Chem.*, 1996, **35**, 6892-6898.
31. S. Y. Dong, Menage, B. A. Brennan, T. E. Elgren, H. G. Jang, L. L. Pearce, L. Que, *J. Am. Chem. Soc.*, 1993, **115**, 1851-1859.
32. W. F. Zeng, C. P. Cheng, S. M. Wang, M.-C. Cheng, G.-H. Lee and Y. Wang, *Inorg. Chem.*, 1995, **34**, 728-736.
33. A. K. Boal, J. A. Cotruvo, Jr., J. Stubbe and A. C. Rosenzweig, *Science*, 2010, **329**, 1526-1530.
34. A. K. Boal, J. A. Cotruvo, Jr., J. Stubbe and A. C. Rosenzweig, *Biochemistry*, 2012, **51**, 3861-3871.
35. N. Cox, H. Ogata, P. Stolle, E. Reijerse, G. Auling and W. Lubitz, *J. Am. Chem. Soc.*, 2010, **132**, 11197-11213.
36. Q. Chen, J. B. Lynch, P. Gomez-Romero, A. Ben-Hussein, G. B. Jameson, C. J. O'Connor and L. Que, *Inorg. Chem.*, 1988, **27**, 2673-2681.
37. P. J. Pessiki, S. V. Khangulov, D. M. Ho and G. C. Dismukes, *J. Am. Chem. Soc*, 1994, **116**, 891-897.
38. S. J. Brudenell, L. Spiccia, A. M. Bond, G. D. Fallon, D. C. R. Hockless, G. Lazarev, P. J. Mahon and E. R. T. Tiekink, *Inorg. Chem.*, 2000, **39**, 881-892.
39. P. Gentschev, N. Moller and B. Krebs, *Inorg. Chim. Acta*, 2000, **300-302**, 442-452.
40. I. A. Koval, P. Gamez, C. Belle, K. Selmeczi and J. Reedijk, *Chem. Soc. Rev.*, 2006, **35**, 814-840.
41. J. Kaizer, R. Csonka, G. Baráth and G. Speier, *Transit. Metal Chem.*, 2007, **32**, 1047-1050.
42. Y. Hitomi, A. Ando, H. Matsui, T. Ito, T. Tanaka, S. Ogo and T. Funabiki, *Inorg. Chem.*, 2005, **44**, 3473-3478.
43. C. Eicken, F. Zippel, K. Büldt-Karentzopoulos and B. Krebs, *FEBS Lett.* , 1998, **436**, 293-299.
44. R. Than, A. A. Feldmann and B. Krebs, *Coord. Chem. Rev.*, 1999, **182**, 211-241.
45. M. Merkel, N. Moller, M. Piacenza, S. Grimme, A. Rompel and B. Krebs, *Chemistry*, 2005, **11**, 1201-1209.
46. V. McKee, M. Zvagulis, J. V. Dagdigian, M. G. Patch and C. A. Reed, *J. Am. Chem. Soc.*, 1984, **106**, 4765-4772.